Injectable, pH-responsive hybrid hydrogels for the treatment of periodontitis

Rui Zhu[1], Wenhua Du[1*], Xiaohui Mi[2*]

[1] Department of Stomatology, Affiliated XiaoShan Hospital, Hangzhou Normal University, Hangzhou, 31000, China
[2] Department of Stomatology, Affiliated Tongji University, Shanghai, 20000, China

ARTICLE INFO

ABSTRACT

Anti-inflammatory hydrogels have demonstrated great potential in the treatment of periodontitis. However, intelligent removal of reactive oxygen species (ROS) remains significantly challenging. In this study, a novel pH-responsive anti-inflammatory hydrogel was designed to treat periodontitis. We synthesized methacrylated alginate modified with a unique pH-sensitive phenylboronic acid through a one-step synthesis and then incorporated polydopamine particles loaded with minocycline to obtain a novel hydrogel under ultraviolet irradiation. Infrared and ultraviolet tests confirmed the successful preparation of the hydrogel. In environments with low pH, drug release rates significantly increased. In addition, in vitro cell experiments demonstrated excellent biocompatibility of the hydrogels. Furthermore, ROS detection revealed that the hydrogel effectively reduced cellular ROS levels and displayed excellent anti-inflammatory properties. These results strongly suggest that this novel pH-responsive anti-inflammatory hydrogel platform has tremendous potential for the treatment of periodontitis.

Introduction

Periodontitis is an inflammatory response of periodontal tissues to the microbiota, characterized by the loss of periodontal attachment, eventually leading to tooth loss (1-3). Periodontal therapy halts disease progression and resolves inflammation by eliminating the microbiota. Mechanical debridement using either manual or power-driven instruments is the primary means of removing supragingival and subgingival deposits from root surfaces (4). In most cases, clinical parameters improve following this gold-standard non-surgical therapy. However, in certain situations, non-surgical mechanical therapy may not completely remove the pathogenic microbiota in the subgingival region, such as in the case of microbial communities invading the periodontal tissues or residing in deep periodontal pockets, which severely impairs periodontal therapy and the healing process. In non-surgical periodontal therapy, microbial biofilms are minimized or eliminated using mechanical and chemotherapeutic methods. Several chemotherapeutic methods are used to prevent plaque from accumulating and to disinfect the periodontal tissues and root surfaces. This is accomplished through the local application of various antimicrobial agents or drugs that are used to deliver local nidus over a prolonged period. Plaque removal in deep pockets may not be possible through mechanical therapy, leading to treatment failure as bacterial plaque accumulates post-therapy. Therefore, combining mechanical therapy with chemotherapeutic agents is a critical approach to periodontitis treatment.

Recently, in situ polymerized hydrogel systems have garnered significant interest because of their exceptional adhesive properties and drug release profiles under controlled conditions (5). These systems are particularly effective in periodontal applications because they offer advantages over traditional delivery systems. In situ systems typically comprise mixtures of intelligent polymers with stimuli-responsive properties that transition from the solid state to the gel state upon contact with some biological stimulation, such as changes in pH, solvent composition, ion concentration, and temperature (6). Despite the immense advantages and potential of in situ gel systems, there are limitations in selecting appropriate polymers, complex formulation systems, and utilizing polymer concentrations to provide the desired drug release profiles for prolonged periods. Furthermore, efficacious treatment for periodontitis needs the maintenance of drug concentration in the periodontal pocket above the minimum inhibitory concentration (MIC); this necessitates the development of an effective periodontitis formulation system. In this regard, the use of biodegradable polymer nanoparticles in drug delivery research has been widely explored for controlling drug release profiles ranging from days to weeks and potentially months. Moreover, nanoparticles are considered effective primarily because of their small size, which can help them reach the gingival crevice as well as deep periodontal pockets (7). Therefore, the development of in situ gel formulations loaded with nanoparticle cargo that transition from a sol state to a gel state upon contact with human periodontal tissue has been devised to extend its residence time in the periodontal pocket (8).

To date, various drugs with antibacterial, antioxidant, and anti-inflammatory properties have been used to treat periodontitis. Boric acid (BA) is one such drug that has recently been evaluated for its use in locally treating chronic periodontitis (9). BA and borates naturally occur as boron and possess many metallic and nonmetallic properties. It has been reported that boron possesses antibacte-

rial properties; furthermore, it regulates inflammation and immune response. In 2014, a study showed that BA could alleviate the inflammation and alveolar bone loss associated with diabetic periodontitis induced by ligatures (10). BA exhibits antibacterial and anti-inflammatory properties due to the presence of boron (11). This compound reduces the release of tumor necrosis factor-alpha (TNF-α) by lipopolysaccharide-induced human monocytes, endowing BA with anti-inflammatory and antibacterial properties. BA also increases osteogenic activity by stimulating the synthesis of bone formation-related marker genes in human bone marrow stromal cells during their proliferation and differentiation cycles. The structural basis of the boric acid ester bond is an ester bond formed dynamically by boric acid and cis-diol, which is applied extensively in medicine for regenerative processes and drug delivery. In addition, B-N coordination bonds formed between boron atoms and secondary amines can increase hydrolytic stability (12). A combination of mechanical viscoelasticity and controlled arginine release can be achieved by incorporating arginine into borate hydrogels (13).

Therefore, to satisfy the complex environmental requirements for treating periodontitis, we have designed a pH-responsive hydrogel material. First, we covalently modify phenylboronic acid (PBA) onto methacrylated alginate (AlgMA) through an amidation reaction under the action of N-(3-Dimethylaminopropyl)-N′-ethylcarbodiimide hydrochloride (EDC) and N-Hydroxysuccinimide (NHS). Subsequently, polydopamine particles loaded with gentamicin were added. Finally, the hydrogel was rapidly formed under ultraviolet (UV) irradiation. Boronate-based hydrogel materials can break down in the low-pH region of inflammation, thereby accelerating drug release; meanwhile, rapid UV polymerization can meet the requirements of special wound sites by concentrating the drug at the wound site. In vitro experiments show that this hydrogel significantly increases the drug release rate in a low-pH environment, effectively inhibiting inflammation. In addition, this hydrogel is nontoxic to living organisms and is worthy of further clinical application.

Materials and Methods

Reagents and chemicals

AlgMA was provided by Macklin (China). PBA, EDC, NHS, 2-(N-morpholino) ethanesulfonic acid hydrate (MES), and dopamine (DA) were supplied by Aladdin (China). The α-minimum essential medium (α-MEM) and phosphate-buffered saline (PBS) were sourced from Hyclone (USA). In addition, fetal bovine serum (FBS) was brought from Gibco (USA), and cell counting kit-8 (CCK-8) was obtained from Beyotime (China).

Characterization of hydrogel

Fourier-transform infrared spectroscopy was applied to elucidate the chemical structure of the polymer. A Malvern Zetasizer Nano-ZS90 instrument (Malvern, UK)

was utilized to detect zeta potential and size distribution. Scanning electron microscopy (SEM, Hitachi, Japan) was employed to visualize the structures of freeze-dried hydrogels as well as micelles. The micelle shapes were observed by transmission electron microscopy (Hitachi, Japan). Furthermore, the loading efficiency of the drugs into the hydrogel was evaluated by a UV-Vis spectrophotometer (Shimadzu, Japan).

Synthesis of AlgMA-PBA/PDA@Gentamicin (APPG)

Preparation of AlgMA-PBA

AlgMA-PBA was synthezised via the esterification of AlgMA and PBA. In short, AlgMA (1 g) was solubilized in MES buffer (0.1 M) to make a 1% solution. Next, 5 mL of 1% PBA dissolved in dimethyl sulfoxide was added. After thorough dissolution, EDC (0.5 g) and NHS (0.5 g) were added, and the mixture was stirred at room temperature (RT) for 24 h. The mixture was then centrifuged to dislodge any non-reacted PBA. At last, the supernatant (MWCO 3500) was dialyzed for 5 d using deionized water and freeze-dried.

Preparation of PDA

Then, ammonia (3 mL) was added to a mixture containing 90 mL of deionized water and 40 mL of anhydrous ethanol to modulate the pH value to 8.5. Afterward, the solution was stirred for 0.5 h at RT. Next, Dopamine hydrochloride (0.5 g) was added to the mixture and dissolved thoroughly. The solution was stood for 24 h before undergoing centrifugation to collect the precipitate. After washing, the PDA was dried in a freeze-dryer for 24 h and then stored for further use.

Preparation of AlgMA-PBA/PDA@Gentamicin (APPG)

To construct the APPG hydrogels, different concentrations of AlgMA-PBA and PDA@Gentamicin were mixed with 1% Irgacure (v/v) 2959. The mixture was then irradiated with UV light for 10 s to form the hydrogel. The details about the composition of each sample are exhibited in Table 1.

Rheological testing of hydrogel

Rheological testing was performed at 37°C by a rotational rheometer (Anton Paar, Austria). A syringe was used to mix the hydrogel uniformly before injecting 0.2 ml onto the rheometer plate. To reduce the rotor height, the plate distance was reduced by 1 mm and the surrounding hydrogel was removed. The storage (G′) and loss (G″) moduli of different APPG hydrogels were studied by frequency sweep in the range of 50–0.1 rad/s and 1% strain amplitude.

Drug release from hydrogel

The effect of gentamicin release was measured by ultraviolet absorbance. We took 0.1 g APPG hydrogel and dissolved it in 10 mL buffer (pH=4.5 and 7.2) at 37°C and

Table 1. Proportion of different components in the sample prepolymer.

Sample	AlgMA-PBA (%)	PDA@Gentamicin (%)	Irgacure2959(%)
APPG-1	10	15	1
APPG-2	10	10	1
APPG-3	10	5	1

100 rpm Fresh buffer was added at every time point, followed by the collection of 1 mL of the supernatant. A UV spectrophotometer was employed to detect the concentration of gentamicin in hydrogels at λ=280 nm. The concentration of gentamicin released from hydrogels was calculated using a standard curve.

Isolation and culture of human periodontal ligament fibroblasts

Five healthy individuals (15-25 years old) provided healthy human premolars for the study. Periodontal tissues were harvested from the roots and cultured in α-MEM containing 5% FBS as well as 0.5% penicillin/streptomycin. Informed consent was obtained from all subjects.

Identification of human periodontal ligament fibroblasts

Vimentin is a marker of fibroblasts, and keratin is a marker of epithelial cells. A 12-well plate was seeded with HPDLCs and the slices were allowed to climb. After pretreatment, the cells were treated with 4% fixative and permeabilized with 0.5% Triton X-100 in PBS. After blocking in 5% BSA, the cells were acted overnight at 4°C with primary antibodies at the dilution of 1:250. Upon DAPI staining, the cells were hatched with secondary antibodies for another 1 h. Finally, ImageJ was applied to quantify the mean fluorescence intensity of proteins.

Live/dead staining

The medium in the plate was discarded and washed. Then, the gel was introduced to the well-plate that had formed the membrane followed by an incubation at 37°C. The well plate was taken out at pre-set time intervals (24 and 48 h), and the gel imparted with the cells was collected. After that, PBS (1 mL) was added to each well, and then 5 μL of fluorescein diacetate (FDA) and propidium iodide (PI) were added to each well to stain the cell membranes. After staining in the dark for 3 min under a fluorescence microscope, cells were observed and photographed.

Cytotoxicity assay

Using a CCK-8 assay kit, the cytotoxicity of the hydrogels was assessed. We discarded the culture medium and added 3 mL of trypsin after washing with PBS, and the cells were incubated at 37°C. Following centrifugation, cell suspensions were cultivated in 12-well culture dishes at 37°C in 5% CO_2. Next, 10 mL FBS was added to 90 mL supernatant, and the solution was carefully transferred to a new 96-well plate. After incubation at 37°C for 24 or 48 h, each well was added with CCK-8. After 4 h, a Multiskan FC Microplate Reader (Thermo, US) was utilized to count cell viability at 450 nm based on the following equation:

$$\text{Cell viability} = \frac{AT - A0}{AC - A0} \times 100\%$$

AT (sample groups), A0 (control group); AC (blank group)

Reactive oxygen species

The antioxidant activity of the APPG hydrogel was detected using the ROS assay kit. First, HPDLCs were cultured in α-MEM with H_2O_2 for 12 h. The hydrogel extract was then added to the medium and incubated for another 12 h. Afterward, the HPDLCs were stained with a DCFH-DA solution (10 μM) for 20 min. Finally, images were acquired with a fluorescence microscope.

Western Blotting

Upon washing, cells were lysed using RIPA buffer (Beyotime, China), loaded and run on a 10% sodium dodecyl sulfate-PolyacrylamideGel Electrophoresis, and transferred to Polyvinylidene difluoride membranes (Millipore, USA). After blocking with 5% non-fat milk, the membranes were probed by the primary antibodies against IL-10 (ab133575, Abcam, China) at 1:1,000 overnight at 4°C. On the second day, the membrane reacted with secondary antibodies. Thereafter, the protein blots were developed and β-actin was served as a control.

Scratch assay

HPDLCs were cultured to 90% confluence and marked with a horizontal line for image acquisition in 6-well plates. After scratching the cells with a 10-l pipette tip, the plates were washed carefully to remove the dislodged cells before being cultured in 4% FBS/α-MEM for 48 h. By using ImageJ software (National Institutes of Health, USA), cells were photographed, and the width of cell-free regions was quantified.

Statistical analysis

The analysis of the study was conducted by SPSS V19.0, and the calculated results were shown as means±SD. Multiple group comparisons were examined using one-way ANOVA and Tukey tests. In addition, the Kruskal-Wallis H test was utilized when the variances were not homogeneous. A statistically significant result was defined as $P < 0.05$ in all cases.

Results

Synthesis and characterization of the polymer

The carboxyl groups were activated using EDC and NHS and the BA moiety was introduced into the AlgMA skeleton (Figure 1).

A new peak was shown at 1670 cm^{-1} in the infrared spectrum as the C=O stretching vibration of the amide bond (Figure 2A). Similarly, the bending vibration of the phenyl ring carbon-carbon double bond was observed at 1500-1600 cm^{-1}, whereas the B-O stretching vibration of the boronic acid moiety occurred at 1340 cm^{-1}. Additionally, the C-H bending vibration of the BA phenyl group was observed at 700 cm^{-1}. The UV spectrum of PDA@Gen showed a clear absorption peak at 280 nm, indicating the successful loading of the drug (Figure 2B). The zeta potential of the APPG was shown in Figure 2C, and the zeta potential value after loading drugs was less than -22.6 mV. Polymers and micelles were successfully prepared,
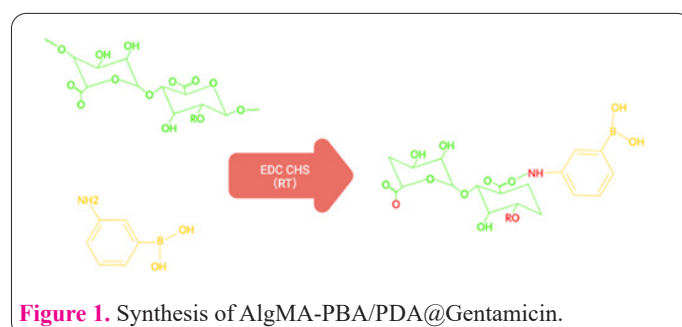

Figure 1. Synthesis of AlgMA-PBA/PDA@Gentamicin.

confirming their effectiveness for preparing drug-containing micelle hydrogels.

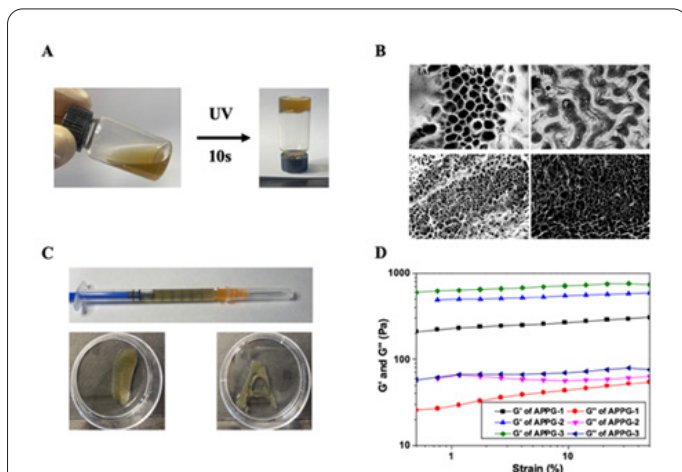## Preparation and characterization of the hydrogel

The purpose of this test was to determine if the APPG solution would form a hydrogel. The pre-polymer solution was placed under a UV lamp, and it was notable to find that a hydrogel could be formed in just 10 s. Photographs captured before and after in situ gelation are shown in Figure 3A. SEM was used to determine the hydrogels' porosity as well as surface structure, which exhibited a uniform porous structure (Figure 3B). As shown in Figure 3C, the APPG hydrogel exhibited injection and reshaping characteristics. As shown in Figure 3D, the G' and G″ of all groups was shown in Figure 3D.

## pH-responsive behavior and drug release of hydrogels

As shown in Figure 4A, the collapse of the hydrogel was induced by the pH-dependent dissociation of the boronic ester bonds between the polymer chains after the pH of the solution was adjusted to 4.5. The release of gentamicin sulfate varies at different pH values; this is consistent with previous reports on the pH-responsive behavior of boronic ester bonds. Specifically, up to 45.6% of gentamicin sulfate was released in the first 24 h at pH 4.5 and was continuously released in the subsequent 24 h, whereas less
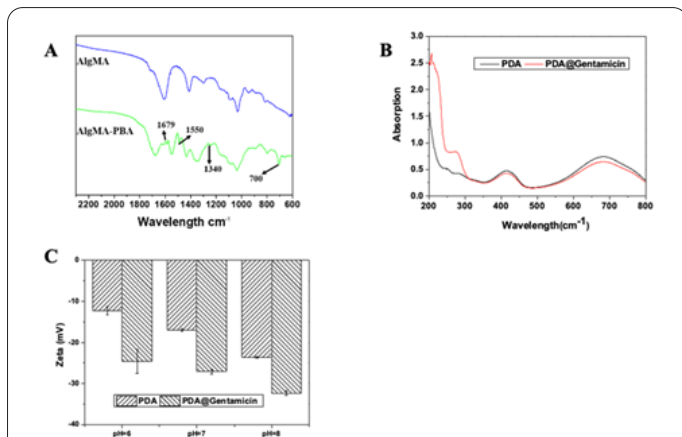

Figure 2. The characterization of the polymer; (A)Infrared spectrum of AlgMA and AlgMA-PBA. (B) UV spectrum of PDA and PDA@Gen. (C) Zeta potential of PDA and PDA@Gen at different pH.

Figure 3. The characterization of the hydrogel; (A) Hydrogel phase transitions by UV. (B) SEM images of APPG hydrogel. (C) the injection and reshaping characteristics of APPG hydrogel. (D)the storage modulus (G′) and loss modulus (G″) of APPG hydrogels.
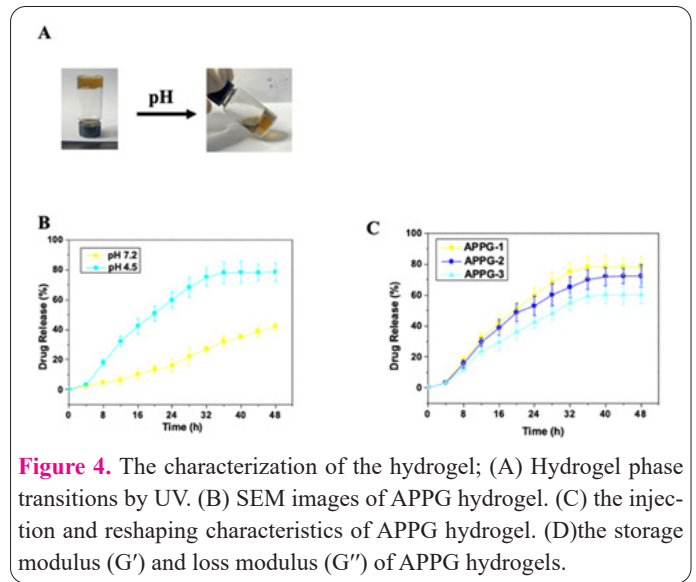
Figure 4. The characterization of the hydrogel; (A) Hydrogel phase transitions by UV. (B) SEM images of APPG hydrogel. (C) the injection and reshaping characteristics of APPG hydrogel. (D)the storage modulus (G′) and loss modulus (G″) of APPG hydrogels.
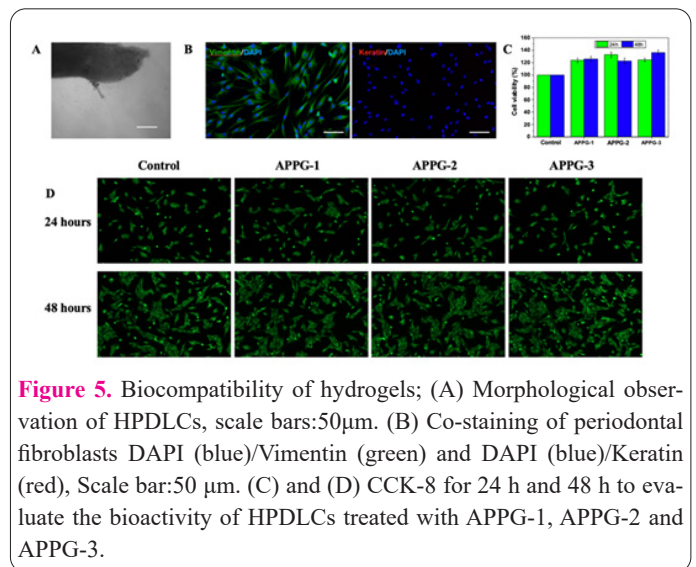
Figure 5. Biocompatibility of hydrogels; (A) Morphological observation of HPDLCs, scale bars:50μm. (B) Co-staining of periodontal fibroblasts DAPI (blue)/Vimentin (green) and DAPI (blue)/Keratin (red), Scale bar:50 μm. (C) and (D) CCK-8 for 24 h and 48 h to evaluate the bioactivity of HPDLCs treated with APPG-1, APPG-2 and APPG-3.

than 40% of gentamicin was released within 48 h at pH 7.2 (Figure 4B). Figure 4C showed the APPG Hydrogels with varying compositions for the release of the drug.

Biocompatibility of hydrogels

HPDLCs culture and identification were successful (Figure 5A and 5B). The proliferation of HPDLCs at 24 and 48 h was exhibited in Figures 5C and 5D.
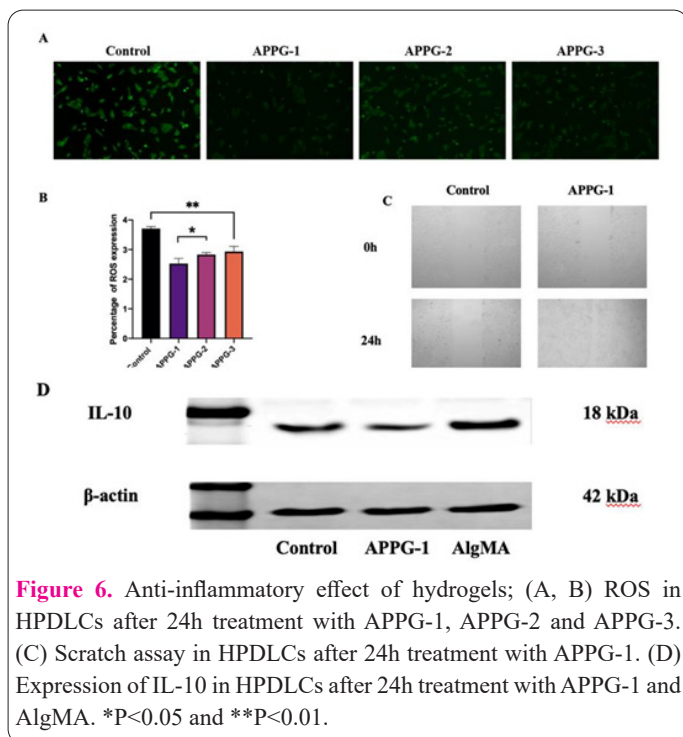
Anti-inflammatory effect of hydrogels

The viability of the HPDLCs was unaffected when co-cultured with APPG-1, APPG-2, or APPG-3 for 48 h. HPDLCs were cocultured with APPG for 24 h to assess their capacity to clear ROS. The results of the experiment are shown in Figure 6A and 6B.

To determine whether the hydrogels affected cell viability and migration, a scratch assay was performed. To calculate the wound closure rate, images of scratched cells were captured at 0 and 24 h (Figure 6C).

As shown in Figure 6D, the level of IL-10 expression was observed in the APPG-1 hydrogels and the control hydrogels (AlgMA).

Discussion

It has been reported that approximately 50% of adults

Figure 6. Anti-inflammatory effect of hydrogels; (A, B) ROS in HPDLCs after 24h treatment with APPG-1, APPG-2 and APPG-3. (C) Scratch assay in HPDLCs after 24h treatment with APPG-1. (D) Expression of IL-10 in HPDLCs after 24h treatment with APPG-1 and AlgMA. *P<0.05 and **P<0.01.

in the U.S. is affected by periodontitis, with 20% having moderate, and 10% severe periodontitis (14). However, there are few therapeutic options for periodontitis. In this study, we developed a kind of injectable, pH-responsive hybrid hydrogel and found the hydrogel has tremendous potential for the treatment of periodontitis.

The UV spectrum of PDA@Gen of hydrogels indicated the successful loading of the drug and the zeta potential value after loading drugs was less than -22.6 mV. Polymers and micelles were successfully prepared, confirming their effectiveness for preparing drug-containing micelle hydrogels. The result of SEM and hydrogel phase transitions by UV showed the dynamic bond rearrangement within the APPG hydrogel occurred at the molecular level, which is different from the typical rigid covalent network-based hydrogels. Therefore, the formation-disruption cycle of dynamic bonds may lead to many unique properties of the hydrogel, such as self-healing (15). Injectable hydrogels were widely used in therapy such as periodontitis and tendon and ligament tissue engineering (16, 17). Hydrogel can be formed into different letters, such as "A" or "1," indicating that the hydrogel is injectable and liquid (18). Due to reversible bond rearrangement, the fabricated hydrogel can be easily molded into shapes such as clock towers and hearts. The G' and G'' of the hydrogel were measured at different frequencies and strain test models were used to investigate its dynamic mechanical properties. As shown in Figure 3D, the G' of all groups of hydrogels was greater than their G″, indicating that the hydrogel had formed (19, 20).

Owing to the pH-responsive boronic ester bond, the sustained-release effect of the hydrogels varies at different pH values (21). Owing to the pH-responsive boronic ester bond, the sustained-release effect of the hydrogels varies at different pH values (21). In addition, we investigated the sustained-release behavior of hydrogels with different compositions and found that the release of drugs decreased with decreasing PDA content at the same time point. Periodontitis is initiated by bacterial plaque and involves the adhesion of microorganisms and the formation of biofilms on the tooth surface and in the periodontal pockets. During glucose fermentation, the pH in the biofilm matrix falls rapidly to 5.0 or below, leading to a consistently low-pH environment in plaque biofilms (22). Acid-tolerant organisms thrive in dental niches in low-pH environments because they disrupt microbial homeostasis (23). pH-responsive hydrogels were successfully synthesized for the controlled release of drugs from periodontitis pockets.

Biological safety, particularly biocompatibility, is crucial for newly developed biomaterials (24). The result of CCK8 indicated that none of the hydrogels showed any inhibitory effect on the growth of fibroblasts after co-culturing for 24 and 48 h. These results demonstrated the good biocompatibility of the hydrogels for biomedical applications.

Wound healing requires specific cellular and molecular mechanisms (25). Wound healing is facilitated by inflammatory cells that mobilize defenses based on local and systemic factors, and the production of several inflammatory cytokines is also important for injury repair (26, 27). HPDLCs were preactivated with TNF to mimic an inflammatory environment. In the microenvironment, pH decreased and ROS levels increased owing to the increased activity of cells after TNF activation, so the dual-responsive hydrogel could demonstrate its anti-inflammatory properties. A large amount of ROS is generated at the site of inflammation in patients with periodontitis, hindering wound healing (28, 29). The green fluorescence signal of ROS in the APPG hydrogel group was significantly decreased, indicating that the hydrogel effectively cleared ROS inside the cells, and APPG-1 had the strongest capacity to inhibit ROS production. We detected the anti-inflammatory and wound-healing capacities of APPG-1 using western blotting and scratch assays. The result showed that cell growth and migration were slower in the control groups but faster in the hydrogel APPG-1 groups. Substantial evidence shows that IL-10 is closely related to periodontitis (30, 31). As shown in Figure 6D, a significantly lower level of IL-10 expression was observed in the APPG-1 hydrogels than in the control hydrogels (AlgMA).

We have developed a novel pH-responsive hydrogel, APPG, for the treatment and healing of periodontitis. The hydrogel exhibits excellent biocompatibility and enables rapid UV polymerization. It not only meets the demands of a complex oral environment but also exhibits pH responsiveness. In low-pH areas of oral inflammation, the hydrogel can accelerate drug release, greatly enhancing the efficacy of the medication. Furthermore, the APPG hydrogel also exhibits anti-inflammatory effects by effectively reducing ROS levels and alleviating inflammation. Further experiments have demonstrated that inflammatory factors can be reduced and cell migration can be promoted by the created hydrogels. Overall, our novel pH-responsive hydrogel platform has tremendous potential for periodontitis treatment.

Interest conflict
The authors declare that they have no competing interests.

Consent for publications

The author read and proved the final manuscript for publication.

Availability of data and material

All data generated during this study are included in this published article.

Authors' contribution

Conceptualization, Xiaohui Mi; Methodology, Xiaohui Mi; Software, Rui Zhu; Formal Analysis, Rui Zhu; Resources, Xiaohui Mi; Writing-Original Draft Preparation, Rui Zhu; Writing-Review and Editing, Rui Zhu; Visualization, Rui Zhu; Supervision, Xiaohui Mi; Project Administration, Xiaohui Mi; Funding Acquisition, Xiaohui Mi. All authors have read and agreed to the published version of the manuscript.

Funding

Ethics approval and consent to participate

Informed consent was obtained from all subjects.

References

1. Tonetti MS, Greenwell H, Kornman KS. Staging and grading of periodontitis: Framework and proposal of a new classification and case definition. J Clin Periodontol 2018;89:S149-S161. DOI: 10.1111/jcpe.12945.

2. Hajishengallis G. Interconnection of periodontal disease and comorbidities: Evidence, mechanisms, and implications. Periodontol 2000 2022;89:9-18. DOI: 10.1111/prd.12430.

3. Ma KS, Wu MC, Thota E, et al. Tonsillectomy as a risk factor of periodontitis: A population-based cohort study. J Periodontol 2022;93:721-731. DOI: 10.1002/jper.21-0215.

4. Bao X, Zhao J, Sun J, Hu M, Yang X. Polydopamine Nanoparticles as Efficient Scavengers for Reactive Oxygen Species in Periodontal Disease. ACS Nano 2018;12:8882-8892. DOI: 10.1021/acsnano.8b04022.

5. Hu C, Zhang F, Long L, et al. Dual-responsive injectable hydrogels encapsulating drug-loaded micelles for on-demand antimicrobial activity and accelerated wound healing. J Control Release 2020;324:204-217. DOI: 10.1016/j.jconrel.2020.05.010.

6. Yang J, Zeng W, Xu P, et al. Glucose-responsive multifunctional metal-organic drug-loaded hydrogel for diabetic wound healing. Acta Biomater 2022;140:206-218. DOI: 10.1016/j.actbio.2021.11.043.

7. Pettignano A, Grijalvo S, Häring M, et al. Boronic acid-modified alginate enables direct formation of injectable, self-healing and multistimuli-responsive hydrogels. 2017;53:3350-3353. DOI: 10.1039/c7cc00765e.

8. Cieplik F, Deng D, Crielaard W, et al. Antimicrobial photodynamic therapy - what we know and what we don't. Crit Rev Microbiol 2018;44:571-589. DOI: 10.1080/1040841x.2018.1467876.

9. Shalehin N, Hosoya A, Takebe H, Hasan MR, Irie K. Boric acid inhibits alveolar bone loss in rat experimental periodontitis through diminished bone resorption and enhanced osteoblast formation. J Dent Sci 2020;15:437-444. DOI: 10.1016/j.jds.2019.09.009.

10. Bashir NZ, Krstic M. Boric acid as an adjunct to periodontal therapy: A systematic review and meta-analysis. Int J Dent Hyg 2021;19:139-152. DOI: 10.1111/idh.12487.

11. Mitruț I, Scorei IR, Manolea HO, et al. Boron-containing compounds in Dentistry: a narrative review. Rom J Morphol Embryol 2022;63:477-483. DOI: 10.47162/rjme.63.3.01.

12. Zhang X, Li Z, Yang P, et al. Polyphenol scaffolds in tissue engineering. Mater Horiz 2021;8:145-167. DOI: 10.1039/d0mh01317j.

13. Sağlam M, Hatipoğlu M, Köseoğlu S, Esen HH, Kelebek S. Boric acid inhibits alveolar bone loss in rats by affecting RANKL and osteoprotegerin expression. J Periodontal Res 2014;49:472-479. DOI: 10.1111/jre.12126.

14. Ilievski V, Toth PT, Valyi-Nagy K, et al. Identification of a periodontal pathogen and bihormonal cells in pancreatic islets of humans and a mouse model of periodontitis. 2020;10:9976. DOI: 10.1038/s41598-020-65828-x.

15. Liang Y, He J, Guo B. Functional Hydrogels as Wound Dressing to Enhance Wound Healing. ACS Nano 2021;15:12687-12722. DOI: 10.1021/acsnano.1c04206.

16. Liu R, Zhang S, Chen X. Injectable hydrogels for tendon and ligament tissue engineering. J Tissue Eng Regen Med 2020;14:1333-1348. DOI: 10.1002/term.3078.

17. Zhao X, Yang Y, Yu J, et al. Injectable hydrogels with high drug loading through B-N coordination and ROS-triggered drug release for efficient treatment of chronic periodontitis in diabetic rats. Biomaterials 2022;282:121387. DOI: 10.1016/j.biomaterials.2022.121387.

18. Lu Y, Qu X, Zhao W, et al. Highly Stretchable, Elastic, and Sensitive MXene-Based Hydrogel for Flexible Strain and Pressure Sensors. Research (Wash D C) 2020;2020:2038560. DOI: 10.34133/2020/2038560.

19. Wang Z, Zhang Y, Yin Y, et al. High-Strength and Injectable Supramolecular Hydrogel Self-Assembled by Monomeric Nucleoside for Tooth-Extraction Wound Healing. Adv Mater 2022;34:e2108300. DOI: 10.1002/adma.202108300.

20. Bayón-Fernández A, Méndez-Ardoy A, Alvarez-Lorenzo C, Granja JR, Montenegro J. Self-healing cyclic peptide hydrogels. J Mater Chem B 2023;11:606-617. DOI: 10.1039/d2tb01721k.

21. Lee SY, Yang M, Seo JH, et al. Serially pH-Modulated Hydrogels Based on Boronate Ester and Polydopamine Linkages for Local Cancer Therapy. ACS Appl Mater Interfaces 2021;13:2189-2203. DOI: 10.1021/acsami.0c16199.

22. Paes Leme AF, Koo H, Bellato CM, Bedi G, Cury JA. The role of sucrose in cariogenic dental biofilm formation--new insight. J Dent Res 2006;85:878-887. DOI: 10.1177/154405910608501002.

23. Peacock ME, Arce RM, Cutler CW. Periodontal and other oral manifestations of immunodeficiency diseases. Oral Dis 2017;23:866-888. DOI: 10.1111/odi.12584.

24. Josyula A, Parikh KS, Pitha I, Ensign LM. Engineering biomaterials to prevent post-operative infection and fibrosis. Drug Deliv Transl Res 2021;11:1675-1688. DOI: 10.1007/s13346-021-00955-0.

25. Wilkinson HN, Hardman MJ. Wound healing: cellular mechanisms and pathological outcomes. Open Biol 2020;10:200223. DOI: 10.1098/rsob.200223.

26. Huang C, Dong L, Zhao B, et al. Anti-inflammatory hydrogel dressings and skin wound healing. Clin Transl Med 2022;12:e1094. DOI: 10.1002/ctm2.1094.

27. Ban E, Jeong S, Park M, et al. Accelerated wound healing in diabetic mice by miRNA-497 and its anti-inflammatory activity. Biomed Pharmacother 2020;121:109613. DOI: 10.1016/j.biopha.2019.109613.

28. Sui L, Wang J, Xiao Z, et al. ROS-Scavenging Nanomaterials to Treat Periodontitis. Front Chem 2020;8:595530. DOI: 10.3389/fchem.2020.595530.

29. Wang Y, Song Y, Zhong Q, et al. Suppressing ROS generation by

apocynin inhibited cyclic stretch-induced inflammatory reaction in HPDLCs via a caspase-1 dependent pathway. Int Immunophar-macol 2021;90:107129. DOI: 10.1016/j.intimp.2020.107129.

30. Chen X, Wan Z, Yang L, et al. Exosomes derived from reparative M2-like macrophages prevent bone loss in murine periodontitis models via IL-10 mRNA. J Nanobiotechnology 2022;20:110.

DOI: 10.1186/s12951-022-01314-y.

31. Taiete T, Monteiro MF, Casati MZ, et al. Local IL-10 level as a predictive factor in generalized aggressive periodontitis treat-ment response. Scand J Immunol 2019;90:e12816. DOI: 10.1111/sji.12816.